Int. J. Electrochem. Sci., 15 **(2020)** 5723 – 5740, doi: 10.20964/2020.06.24

International Journal of
ELECTROCHEMICAL
SCIENCE
www.electrochemsci.org

Electrochemical Corrosion Control for Reinforced Concrete Structures–A Review

Bingbing Guo[1,*], *Guofu Qiao*[2], *Ditao Niu*[1], *Jinping Ou*[2]

[1] School of Civil Engineering / Key Lab of Engineering Structural Safety and Durability / National Key Laboratory of Green Building in West China, Xi'an University of Architecture and Technology, Xi'an, 710055, China
[2] School of Civil Engineering / Key Lab of Smart Prevention and Mitigation of Civil Engineering Disasters of the Ministry of Industry Information Technology / Key Lab of Structures Dynamic Behavior and Control of the Ministry of Education, Harbin Institute of Technology, Harbin 150090, China
[*]E-mail: guobingbing212@163.com

Received: 8 January 2020 / *Accepted:* 16 March 2020 / *Published:* 10 May 2020

Electrochemical corrosion control (ECC), including cathodic protection (CP), electrochemical chlorine removal (ECR) and electrochemical realkalisation (ER), is extremely effective for improving the durability of reinforced concrete structures. This paper summarizes recent studies on ECC. The findings indicate that long-term ECC with an intermittent small current can achieve CP, ECR, and ER, making it an attractive approach. It is imperative to develop a numerical model of ECC that includes ionic transport in pore solution, oxygen and water transports, thermodynamic reactions, and electrode kinetics. Additionally, an intelligent system integrating corrosion monitoring and intermittent ECC will be beneficial.

Keywords: reinforced concrete structures; corrosion control; cathodic protection (CP); electrochemical chloride removal (ECR); electrochemical realkalisation (ER)

1. INTRODUCTION

Reinforced concrete (RC) structures are a significant structural style in civil engineering, which are important for the infrastructure construction of any country; they can be applied in super dams, long-span bridges, skyscrapers, etc. Generally, RC structures are expected to function for decades, if not hundreds of years. However, the corrosion of reinforcing steel seriously degrades the service life of RC structures, especially when they are exposed to aggressive environments [1, 2]. For example, in deicing salt or coastal marine environments, chloride can easily penetrate into RC structures owing to

diffusion, convection, electromigration, and capillary suction [3-5]. The passive film at the surface of reinforcing steel is destroyed when the concentration of chloride is higher than the threshold value [6-9]. Additionally, carbonation can lower the pH value of concrete pore solutions, and destroy the passive film [10-12]. With the presence of oxygen and water, the corrosion of reinforcing steel is initiated [9], which not only reduces the effective section area of the reinforcing steel but also causes the cracking of concrete. Ultimately, it results in the rapid descent of the bearing capacity of RC structures, or the collapse of structure [13-15].

Corrosion control is an effective method to improve the durability and safety of RC structures and prolong their service life. In recent decades, many passive and active corrosion control methods for RC structures have been developed [2, 16, 17], such as improving the anti-penetrating performance of concrete, enhancing the corrosion resistance of steel bars, applications of corrosion inhibitors and anti-corrosion coating, cathodic protection (CP), electrochemical chlorine removal (ECR), and electrochemical realkalisation (ER). In nature, the corrosion of reinforcing steel is the dissolution of iron as the anode in an electrochemical cell. In CP, ECR, and ER, an external anode is introduced, and the reinforcing steel functions as a cathode. Subsequently, an electric field is applied into RC structures to provide a CP current for reinforcing steel, remove chloride ions from chloride-contaminated concrete, or improve the alkalinity of carbonated concrete structures. Therefore, electrochemical corrosion control (ECC), i.e. CP, ECR, and ER, is the most direct and effective method to improve the durability of RC structures that are vulnerable to chloride or carbonation attacks [16, 18-23].

In recent years, many researchers have investigated the CP, ECR, and ER of RC structures. Their investigation results indicated that these electrochemical techniques have their own advantages and disadvantages in controlling the corrosion of RC structures [17, 24-27]. Hence, a comprehensive and updated review of recent investigations relating to these three electrochemical techniques in RC structures is presented herein. It should be noted that recent studies regarding the engineering applications of these three electrochemical techniques will be not introduced in this paper, as they are available in [16, 18, 25]. The paper is organised as follows. Sections 2, 3, and 4 summarise recent studies regarding CP, ECR, and ER, respectively. Section 5 introduces the effect of ECC on the material and structure performances of RC. Section 6 discusses and analyses CP, ECR, and ER. Section 7 presents the conclusions.

2. CP

CP refers to corrosion control based on thermodynamics. An external anode is introduced, and a small current is applied onto the protected RC structure. The reinforcing steel serves as a cathode as opposed to the dissolving anode in an electrochemical corrosion cell [25, 26, 28], and hence, the potential of the reinforcing steel is negatively shifted. Owing to the difference in the methods to provide protection current, CP is categorised into impressed current cathodic protection (ICCP) and sacrificial anode cathodic protection (SACP) [29, 30]. In ICCP, an inert anode is used, and the protective current is provided by an external power source [31]. In SACP, a metal anode that is more active than iron is used, such as aluminium, zinc, magnesium, or their alloys, and the protective current

originates from the difference in electrochemical potentials between the anode and iron. Therefore, ICCP is more suitable for large structures with severe corrosion and long-life expectancy, whereas SACP is more suitable for targeted repairs with limited budgets and shorter life expectancies [24]. Table 1 compares their advantages and disadvantages for their applications in RC structures. When CP is applied to a new RC structure, it is known as cathodic prevention. The applied current density in cathodic prevention is much lower than that in CP; in the ISO12696:2016 standard, the suggested applied current density on steel surfaces is 0.2–2.0 mA/m^2 for cathodic prevention, whereas it is 2.0–20 mA/m^2 for CP [32].

Table 1. Comparison between ICCP and SACP [16, 25]

	Advantages	Disadvantages
ICCP	1. Controllable current 2. Commonly used in RC structures 3. Higher life expectancy	1. Require permanent external power source and continuous monitoring 2. Greater risk of hydrogen embrittlement 3. Larger maintenance and management 4. Easily produces interference to adjacent structures
SACP	1. Simpler installation and design 2. No interference to adjacent structures 3. No external power source required 4. No risk of hydrogen embrittlement	1. No availability in higher resistive concrete 2. Unable to control protective current 3. Limited service life

Except the effect of CP on the material and structure performances of RC (presented in Section 5), recent studies regarding CP are primarily related to the anode and its numerical simulation, which will be introduced in the following sections.

2.1 Novel anodes for CP

The anode directly determines the corrosion control efficiency of CP and the service life. For SACP, the activity of the anode must be higher than that of iron, and it is generally composed of zinc, aluminium and magnesium [25]. It can be designed into metallic coating anodes, anode jackets, adhesive zinc sheet anodes, discrete anodes, etc. For ICCP, the anode must exhibit good conductivity, excellent anti-polarisation and a low corrosion rate, e.g. activated titanium, coke breeze asphalt, conductive organic paints, cement-based conductive composites, and carbon fibre reinforced polymer. Among them, cement-based conductive composites and carbon fibre reinforced polymers (CFRPs) have recently been proposed as anodes in ICCP, and they will be reviewed in detailed in this section.

Cement-based materials are non-conductive, and cannot be used as the anode of CP. However, adding some conductive fillers into cement-based materials, e.g. carbon fibre, carbon black, and graphite, not only enables them to exhibit a good conductivity, but can also improve their mechanical properties. Compared with activated titanium meshes, metalised zinc, coke breeze asphalt, and

conductive organic paints, cement-based conductive composites as anode offer significant advantages owing to their excellent compatibility with concrete, low cost and good durability. Hou et al. [33] first studied carbon fibre reinforced mortar and concrete as anodes in ICCP for RC structures, and have verified this possibility. Some experimental investigations [34-40] indicated that cement-based conductive composites could function as anode in ICCP. Bertolini et al. [35] discovered that conductive mortars with the addition of nickel-coated carbon fibres exhibited satisfactory anodic functions for CP although they underwent a current density of up to 20 mA/m^2 for two years. Anwar et al. [37] developed a light-weight cementitious conductive anode that was primarily composed up of pumice aggregates (fine), carbon fibres, and cement. The studies by Xu et al. [36] indicated that the optimum content of carbon fibres should be slightly higher than its conductive percolation threshold in cement-based materials. In addition, Carmona et al. [38] investigated conductive cement pastes with graphite as anodes in ICCP, and found that it could not only control the corrosion well, but could also remove a substantial portion of chloride. Cañón et al. [39], Pérez et al. [40] and Jin et al. [41] verified that using cement conductive composites as anodes could remove chloride in RC structures. However, the long-term operation of ICCP can cause acidification damage of cement-based anodes, and decreases their service life [42, 43]. Guo et al.[44] added lightweight functional aggregates loaded with modified agar gel into cement-based anodes to halt acidification damage. In summary, it has been proven that cement-based conductive composites can be used as anodes in ICCP. Considering that cement-based conductive materials have some other functions, such as the electrothermal effect, pressure sensibility, and electromagnetic shielding effect [45-49], multifunctional cement-based anodes for the ICCP of RC structures should be developed.

CFRPs are a well-known material for retrofitting structures, and exhibit good conductivity [50]. Gadve et al. [51, 52] and Nguyen et al. [53] proposed using CFRPs as anodes in the ICCP of RC structures, and verified its effectiveness in controlling corrosion in laboratory tests. Furthermore, Zhu et al. [54] investigated the electrical and mechanical performances of the CFRPs used as anodes in a simulated ICCP system, and discovered that the performances did not degrade significantly when the current densities of 0.2 and 2 A/m^2 were applied for 25 d. It was predicted that the minimum service life would exceed 12 years, even with the maximum acceptable protection current density [54]. Subsequently, CFRPs have been proposed for both the structural strengthening of corroded RC structures and anodes in ICCP, and this dual function of CFRPs has been verified by experimental results [55-57].

2.2 Numerical model of CP for RC structures

Numerical simulation is useful and effective for investigating the CP of RC structures. Currently, numerical models of CP are based on Laplace equations. At the macro level, concrete can be assumed as a homogeneous conductive material. Hence, the electrolyte domain should obey the law of charge conservation when CP is applied [58, 59]:

$$\nabla \cdot \vec{i} = 0. \quad (1)$$

Here, $\vec{i}$ is the current density vector in concrete.

According to Ohm's law, we can obtain:

$$\vec{i} = -\sigma \nabla \phi, \quad (2)$$

where σ is the conductivity of concrete; ϕ is the electric potential.

In addition, the following boundary conditions at the cathode/anode–concrete interface should be satisfied:

$$\phi^{a,c} = \phi_0{}^{a,c}, \quad (3)$$

$$i^{a,c} = i_0{}^{a,c}, \text{ and} \quad (4)$$

$$i_{a,c} = f(\phi_{a,c}). \quad (5)$$

Here, $\phi^{a,c}$ and $\phi_0{}^{a,c}$ are the potential and initial potential at the cathode/anode–concrete interface, respectively; $i^{a,c}$ and $i_0{}^{a,c}$ are the current density and initial current density at the cathode/anode–concrete interface, respectively. Eqs. (3) and (4) denote the boundaries of the electric potential and current density, respectively, which are determined by the amplitude of the external applied electrical field. Eq. (5) denotes the polarisation boundary, which is determined by electrode reactions at the interfaces [60, 61]. At the cathode–concrete interface, the reduction reaction of oxygen is expected to occur when applying CP. However, iron corrosion may occur when the applied electric field is extremely small and insufficient for completely preventing the corrosion of reinforcing steel; hydrogen evolution may occur when the applied electric field is extremely large. The reaction of oxygen reduction or hydrogen evolution can improve the pH value of the pore solution adjacent to reinforcing steel, which is beneficial for controlling corrosion. However, hydrogen evolution may produce hydrogen and easily causes hydrogen embrittlement, in particular in pre-stressed RC structures [60]. At the anode–concrete interface, some acidification reactions may occur, such as $4OH^- - 4e^- \rightarrow 2H_2O + O_2$, or $2Cl^- - 2e^- \rightarrow Cl_2$ (if concrete is contaminated by chloride). However, some anodes are designed to only evolve oxygen, e.g. mixed-metal-oxide-coated titanium anodes. In numerical simulations, Tafel equations [60, 62, 63] or the measured polarisation curves [59, 61, 64, 65] are generally used to express the polarisation boundaries (Eq. (5)).

According to the theory above, a numerical simulation based on the finite element method (FEM) [58-62, 65, 66] or boundary element method [64] was developed to investigate the CP of RC structures. In these numerical investigations, the effects of external environmental conditions (e.g. chloride concentration, oxygen concentration, and moisture) and internal factors (e.g. amplitude of the applied electric filed, position and geometry of anode, resistance of concrete, and arrangement of reinforcement) on the distributions of current density and electric potential at the steel surface were investigated and discussed. The results indicated that these factors significantly affected the efficiency of CP.

Designing a CP system for RC structures is to ensure the amplitude of the applied electric field and the type, position, geometry and size of the anode. Hence, Qiao et al. [61] proposed a numerical optimisation method, by which the optimal scheme of ICCP for RC structures can be obtained. The optimised variables were the amplitude of the applied electric field, and the position and area of cement-based anodes. The optimisation objective was to minimise the total cost of an ICCP system, which included the initial investment cost to build it and the cost to maintain its normal operation. The former was converted into the construction cost for coating one square metre of cement-based anode,

and the latter was converted into the cost of consumed electricity. Hence, the objective function was obtained as follows:

$$\min f(x_1, y_1, z_1, x_2, y_2, z_2, \ldots x_n, y_n, z_n, S_1, S_2, \ldots, S_n, u)$$
$$= T_1 \cdot u \cdot \left(\sum_{k=1}^{n} \int_{S_k} i_a(x, y, z)\ ds \right) \cdot N + T_2 \sum_{k=1}^{n} \int_{S_k} ds \quad . \qquad (6)$$

Here, n is the number of cement-based anodes; x_1, x_2,..... x_n, y_1, y_2,..... y_n, and z_1, z_2,..... z_n determine the position of the cement-based anode; S_1, S_2,..... S_n are the areas of the cement-based anode; u is the applied voltage for ICCP; i_a (x,y,z) is the anodic current density; T_1 and T_2 are the ICCP operating cost in the RC structure per kilowatt hour consumed and the initial construction cost for coating one square metre of cement-based anode, respectively; and N is the service life of the anode, which is determined by the total charge density that it can survive [37, 67].

In addition, the constraint condition should ensure that the reinforcing steel is completely protected and that the life expectancy of the ICCP system is longer than that of the protected RC structure. Hence,

$$N \geq N_1, \qquad (7)$$

and $$\phi_L \leq \phi_s \leq \phi_U . \qquad (8)$$

Here, N_1 is the life expectancy of the protected RC structure; ϕ_L and ϕ_U are the lower and upper limits of the protection potential, respectively; ϕ_s is the potential at the surface of the reinforcing protected steel.

Based on this numerical optimisation method, the ICCP for a small-scale RC T-shaped beam was designed. Compared with the initial scheme, the total cost of the optimised ICCP system was predicted to decrease by five times during a service period exceeding 50 years [61]. The electric potential and the current density at the steel surface are illustrated in Fig. 1, and the results clearly indicated that the ICCP scheme after the numerical optimisation could completely control the corrosion of the reinforcing steel in a T-shaped beam.

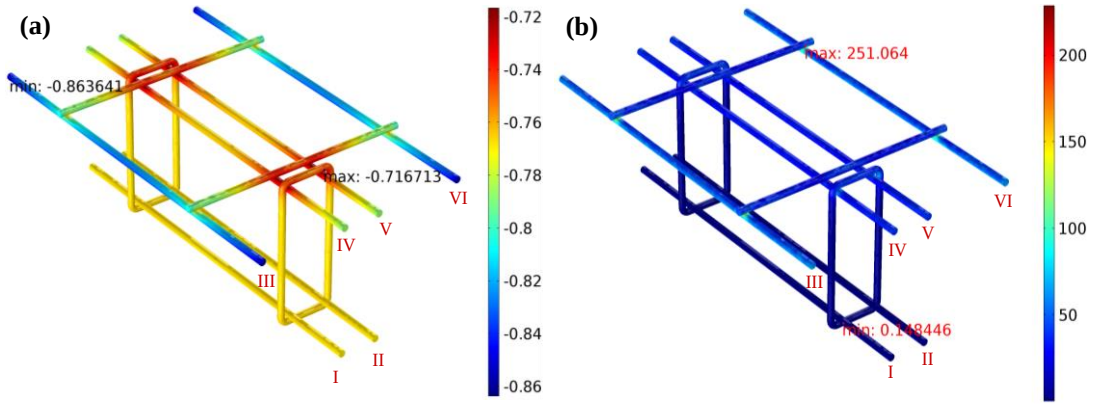

Figure 1. Results of numerical simulation in the optimized scheme: (a) potential of reinforcing steel (V vs.SCE); (b) current density of reinforcing steel (mA/m^2) [61].

This numerical optimisation method is based on the solver of a commercial software, and it has

currently been limited to the application of designing ICCP for small-scale RC components in laboratories. Hence, cloud computing must be employed to conduct the numerical optimisation of ICCP for large-scale RC structures.

3. ECR

Compared with ICCP, a larger external electric field in ECR is applied to force chloride ions in concrete to move into the external electrolyte solution or toward the external anode in a shorter period. ECR is a temporary treatment that aims to lower the chloride concentration in concrete. Except the effect of CP on the material and structure performances of RC (provided in Section 5), most recent studies regarding ECR have discussed the efficiency of ECR with different effects through experimental investigations or numerical simulations, which will be introduced in the following sections.

3.1 Experimental investigations of ECR

External environmental conditions and internal factors directly affect the efficiency of ECR [68], such as temperature, amplitude of applied current density, type of anode, initial chloride concentration in concrete, and initial corrosion state of reinforcing steel.

Temperature affects the activity and diffusivity of free ions in the pore solution and the binding behaviours of cement hydrates for chloride ions. Ueda et al. [69] found that the efficiency of ECR increased by 10% when the temperature increased from 20 °C to 50 °C. Hence, increasing the environmental temperature is a method to improve the efficiency of ECR. An external alkaline electrolyte solution is generally required in ECR, and KOH, LiOH, NaOH, or saturated $Ca(OH)_2$ solutions are used. The efficiency of ECR with different external electrolytes may differ. Hence, Yodsudjai et al. [70] studied the efficiency of ECR using three different external electrolytes, i.e. $Ca(OH)_2$, KOH, and NaOH solutions, and found that it was the highest when $Ca(OH)_2$ solution was used. Huyen Nguyen et al. [71] used Na_3BO_3 solutions as the external electrolyte for ECR, and found its effectiveness. Furthermore, the efficiency of ECR was affected by the water-to-cement ratio of concrete, and the efficiency of ECR for concrete structures with a higher water-to-cement ratio was higher [72, 73]. Additionally, owing to the chloride binding behaviour of cement hydrates, the binder type used in concrete significantly affected the efficiency of ECR. Kim et al. [74] reported that the removal of chlorides in concrete specimens with ground granulated blast furnace slag was more significant than that of ordinary Portland cement. In the study of Garcés et al. [75], ECR was applied to RC structures with four different reinforcing steel arrangements, and it was discovered that the steel arrangements significantly affected the efficiency of ECR. In another study, Change et al. [76] investigated the effect of stirrups on the efficiency of ECR, and discovered that the chloride ions enclosed by a rebar cage were difficult to be removed. In a study by Yeih et al. [77], two different types of anodes were used, i.e. the radial type and the layer type. Their results indicated that the chloride ion

inside the steel cage could be removed using auxiliary electrodes. Saraswathy et al. [78] investigated ECR for RC structures with different anodes, including perforated stainless-steel sheets, titanium meshes, and cement-based conductive composites with carbon fibre; they discovered that cement-based conductive anodes were more suitable for the long-time application of ECR owing to their more stable performances.

In the experiment conducted by Saraswathy et al. [78], it was evident that the efficiency of ECR with the current density of 2.0 A/m^2 was higher than that of ECR with the current density of 1.0 A/m^2; hence, increasing the applied current density can improve the efficiency of ECR [79], but the adverse effect of ECR on RC structures may be more pronounced, which will be discussed in detail in Section 5. In a study by Orellan et al. [80], ECR with the current density of 1 A/m^2 on the steel surface was applied to RC structures for 50 d. Approximately 60% of the initial chloride in concrete and approximately 50% of the chloride adjacent to the steel surface could not be removed. In the experiment conducted by Fajardo et al. [79], ECR with the current density of 1 A/m^2 on the steel surface was applied to the RC cylinder contaminated by chloride for 90 d, And 40%–50% of the initial chloride in concrete could not be removed, whereas chloride ion with 1% cement mass still existed on the steel surface. These results indicated that in all cases, a considerable portion of chloride ions in concrete could not be removed. Chloride in concrete exists either in a pore solution, or is chemically and physically bound to cement hydrates [81]. The relationship between free and bound chlorides is dependent on the physical and chemical equilibriums between the pore solution and cement hydrates [82]. Although the removal of free chlorides in the pore solution contributes to the release of bound chlorides, the rate of the release is lower than the rate of chloride removal. Hence, the efficiency of ECR is lower than expected [83]. In addition, ECR can affect the pore structure and increase the resistivity of concrete, thereby reducing the rate of ionic migration in concrete [84]. Therefore, to some extent, increasing the operation time or the amplitude of applied electric field is not effective for improving the efficiency of ECR. The intermittent ECR method can address this issue, as confirmed experimentally by Saraswathy et al. [78], Elsener et al.[83], and Hai et al.[85]. The current off period allows the new equilibrium between bound and free chlorides to be re-established. The 're-establishing-time' required is 24–48 h, which can be the current off period [83].

Because chloride ions are not required once the corrosion of reinforcing steel is initiated, ECR is considered to be only effective for repairing un-corroded chloride-contaminated RC structures, and is ineffective for highly corroded reinforced concrete structures [27, 68, 86]. Hence, the initial corrosion state of RC structures must be evaluated before performing ECR. Recently, CFRP has been proposed as the anode for ECR [87-90], which is similar to ICCP. This can not only improve the mechanical property of RC structures, but also remove chloride ions in concrete. Therefore, ECR with CFRP anodes may be effective for improving the durability and safety of highly corroded RC structures.

3.2 Numerical model of ECR

A numerical model based on Nernst–Planck equations has been developed to investigate the

ECR of RC structures. The primary ions in a concrete pore solution are K^+, Na^+, Ca^{2+}, SO_4^{2-}, Cl^- and OH^-. Their transports are governed by electromigration, diffusion, and convection, which are expressed as follows:

$$\frac{\partial c_i}{\partial t} = \nabla\left[D_i\left(\nabla c_i + \frac{z_i c_i F}{RT}\nabla \psi \right)\right] - \nu \cdot \nabla c_i + R_i . \quad (9)$$

Here, c_i, z_i and D_i are the concentration (mol/m^3), charge number and diffusion coefficient (m^2/s) of ion i, respectively; F, R and T are the Faraday constant (96485C/mol), gas constant (9.314 J/(mol·K)) and absolute temperature (K), respectively; ψ is the electric potential (V); ν is the flow rate of pore water (m/s), which is zero in saturated concrete structures; and R_i is the source term, which is often neglected.

Chloride binding significantly affects the ionic transport in concrete; hence,

$$\frac{\partial c_{\mathrm{Cl}}}{\partial t} + \frac{(1-p)\rho_{\mathrm{dry}}}{p}\cdot\frac{\partial c_{b\_\mathrm{Cl}}}{\partial t} = \nabla[D_{\mathrm{Cl}}(\nabla c_{\mathrm{Cl}} + \frac{z_{\mathrm{Cl}} c_{\mathrm{Cl}} F}{RT}\nabla\psi)] - \nu\cdot\nabla c_{\mathrm{Cl}}, \quad (10)$$

where p is the porosity of concrete; c_{Cl} is the concentration of free chloride ions in the pore solution (mol/L); $c_{\mathrm{b\_Cl}}$ are the concentrations of bound chloride ions (mol/L of material); and p_{dry} is the density of absolutely dried concrete (kg/m^3). Typically, four types of chloride binding isotherms are used to describe the relationship between free and bound chlorides, i.e. linear, Langmuir, Freundlich, and BET binding isotherms. Owing to numerical complexity, BET binding isotherm is seldom used, whereas the other three binding isotherms are often used [81]. To obtain a good convergence, different binding isotherms are used in different numerical models. In recent years, the thermodynamic equilibrium between pore solution and cement hydrates, including the phase equilibrium of dissolution/precipitation reactions and the surface complexation reactions for ionic adsorption, has been developed to express the relationship between free and bound chlorides [82, 91-93], as well as coupled into the ionic transport model of cement-based materials [94-97]. Therefore, considering that none of the binding isotherms can accurately describe the relationship between free and bound chlorides, the thermodynamic equilibrium should be adopted when simulating ECR, instead of chloride binding isotherms.

Because the pore solution in concrete serves as an electrolyte, the current density in concrete is determined by the ion flux in the pore solution:

$$I = F\sum_{i=1}^{n} z_i\left[D_i\left(-\nabla c_i - \frac{z_i c_i F}{RT}\nabla\psi \right) + \nu\cdot c_i \right] \quad (11)$$

Additionally, the current density in concrete should satisfy the continuity equation,

$$\nabla\cdot I = 0 \quad (12)$$

At the steel-concrete interface, the following electrode reactions may occur,

$$O_2 + 2H_2O + 4e^- \rightarrow 4OH^- \quad (13)$$

$$2H_2O + 4e^- \rightarrow 2OH^- + H_2 \quad (14)$$

A large amount of hydroxyl ions are generated at the steel surface when ECR is applied. In general, the flux of the generated hydroxyl ions is assumed to be proportional to the applied current density [98-107], and this may be reasonable in ECR as the applied electric field is larger. However, when the applied electric field is smaller, nonlinear polarisation boundary conditions must be

considered, such as in ICCP. In addition, the electrode reactions (i.e. Eqs. (13) and (14)) are affected by moisture content and oxygen concentration adjacent to the reinforcing steel [60]. The effect of oxygen concentration is more significant for saturated concrete structures, whereas the effect of moisture content is more significant for concrete structures with low water saturation. Hence, water and oxygen transports should be considered when simulating ECC.

The FEM has been widely used to solve the theoretical model of ECR above. Li and Wang et al. [98-100] simulated the ionic transport in concrete with ECR, and the numerical results indicated that ECR could not only effectively reduce the concentration of chlorides in concrete, but also improve the concentrations of Na^+, K^+ and OH^- adjacent to the reinforcing steel. Additionally, it was found that chloride binding significantly affected the efficiency of ECR, which has also been confirmed in the numerical results reported by Toumi et al [101]. The numerical results reported by Xia et al. [102-104] indicated that temperature and the initial chloride concentration significantly affected the temporal and spatial distributions of ionic concentrations in cement-based materials with ECR. It was concluded that increasing the temperature was effective in improving the efficiency of ECR when the applied electric field could not be improved [102, 103]. In addition, the quantitative relationships between some factors and the efficiency of ECR have been obtained via the numerical model [105], i.e. the time, applied current density, cover-thickness–to-side-length ratio, initial chloride concentration, and ratio of cross-sectional area of reinforcement to cross-sectional area of specimen, some of which are illustrated in Fig. 2. As shown, the efficiency of ECR increased with time or current density; however, this increasing trend decreased gradually, especially for that increasing with time. With increasing initial chloride concentration, the efficiency of ECR decreased slightly.

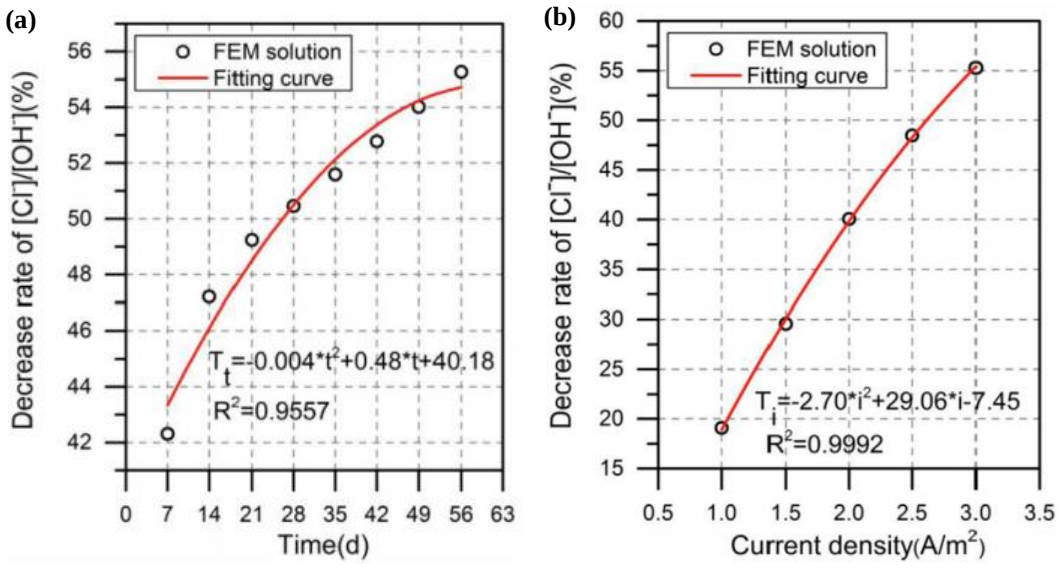

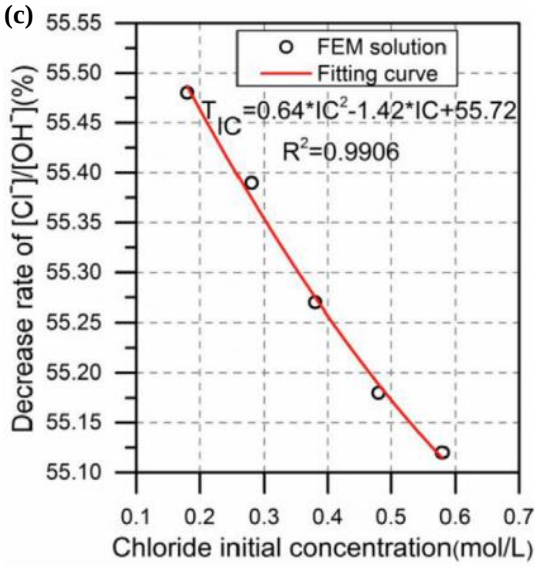

Figure 2. Quantitative relationships between some factors and the efficiency of ECR obtained based on the numerical results: (a) time; (b) current density; (c) initial chloride concentration [105].

In recent years, a multiphase and multicomponent ionic transport mesoscale model has been developed to simulate the ECR of RC structures [106, 107]. Concrete comprises aggregates, interfacial transition zone (ITZ), and cement paste; hence, these three phases were defined using different diffusion coefficients in this model. The location of aggregate was set randomly. The theoretical model based on the Nernst–Planck equation was used, which was solved based on COMSOL.

4. ER

ER is similar to ECR; however, it is used to repair carbonated concrete structures. Generally, a current density of 1–2 A/m^2 with respect to a steel surface can realkalise a concrete cover of several centimetres in a few weeks [108]. The improvement in concrete alkalinity is primarily dependent on the production of OH^- in the electrode reactions and the migration of OH^-. Investigations by Yeih et al. [109] indicated that ER could not only improve the alkalinity of concrete, but also rebuild the passive films at the steel surface. Bertolini et al. [108] proposed using ER to repair historical buildings that have been subjected to long-term carbonation attacks. In their investigations, a current density of 0.8 A/m^2 was applied for 3 weeks to repair the RC columns of a bell tower built in the 1920s. The alkalinity of concrete adjacent to the reinforcing steel improved significantly after ER treatment, and this protection for the RC columns was expected to be maintained for at least several decades. Tong et al. [110] proposed a novel ER treatment, in which an aluminium alloy was applied as a sacrificial anode to produce the protection current. The results indicated that ER could improve the pH value and promote the penetration of alkaline ions. This treatment could not induce any adverse effect on concrete, and the period was extremely long, i.e. at least 12 months.

The amplitude of the applied current density directly determines the efficiency of ER. In general, the pH value and the thickness of the realkalisation concrete can improve with the increase in the applied current density [109]. In addition, some investigations indicated that ER was affected by the water-to-cement ratio, cement type, mineral admixture and thickness of concrete cover [109, 111, 112]. The water-to-cement ratio affects the electric resistance of concrete, and concrete with a higher water-to-cement ratio has a larger electric resistance. Hence, more time and a higher current density are required for ER when water-to-cement ratio is decreased [111, 112]. Cement type and mineral admixture determine the alkalinity of the concrete pore solution; hence, they affect the time and applied electric field of ER [111, 112]. Undoubtedly, ER with a thicker concrete cover requires more time or a larger applied electric field [111].

5. EFFECT OF ECC ON THE MATERIAL AND STRUCTURE PERFORMANCES OF RC

ECC is effective for improving the durability and safety of RC structures; however, it can yield some adverse effects on the performance of RC structures, especially in terms of the properties of concrete and the bonding strength of the steel–concrete interface. By investigating the pore size of concrete before and after ECR, Siegwart et al. [84] found that the pore structure changed significantly, and the concrete resistance increased. In another study [109], the pore structure of concrete after ER was discovered to be denser, and this could affect the ionic migration in the pore solution. Therefore, the impermeability of concrete may increase after ECC treatment, and the efficiency of ECC with increasing time may be lower than expected. Yeih et al. [109] investigated the mechanical properties of carbonated concrete after ER, and the results indicated that both the compressive strength and the elastic modulus decreased. Moreover, some new cementitious phases containing higher concentrations of sodium, aluminium and potassium may be produced after ECR [80], which can contribute to the alkali–silica reaction [113]. In addition, ECC can improve the Na^+, K^+, and OH^- concentrations at the steel surface, and change the concrete microstructure adjacent to the reinforcing steel. Flaherty et al. [114] and Garcia et al. [115] found that the long-term operation of ICCP affected the bonding strength of the steel–concrete interface. However, Flaherty et al. [114] speculated that this effect could be neglected even under the ICCP operation period of 70 years when the applied current density was lower than 0.65 $\mu A/cm^2$. Compared with CP, the applied electric field in ECR and ER was larger, and the effect on the interfacial bonding strength may be more significant. The experimental results by Yeih et al. [109] indicated that the interfacial bonding strength decreased after ER. Zhang and Gong [116], and Guo [117] discovered that the deterioration of the interfacial bonding strength owing to ECR could cause a decrease in the stiffness, ductility and energy dissipation capacity of RC structures. To avoid this adverse effect, Bennett et al. [68] suggested that the current density used in ECR should be less than 5 A/m^2 or 1500 $A{\cdot}hr/m^2$ of the steel surface. In summary, when applying ECC, some ions are produced or consumed at the steel surface owing to electrode reactions, and the free ions in the pore solution are forced to migrate. The ionic migration destroys the existing physical and chemical equilibriums between the pore solution and the hydrate phase. Subsequently, to build new physical and

chemical equilibriums, some ions are released into the pore solution from the hydrate phase, e.g. Cl^-, OH^-, Ca^{2+}, and SO_4^{2-}. The phase assemblages of the cement hydrate are also changed, and in particular, the amounts of monosulfoaluminate, ettringite, Friedel's salt and portlandite tend to be affected. This is reason why ECC can change the pore structure, permeability and mechanical property of concrete, the bonding strength of the steel–concrete interface, and the stiffness, ductility and seismic capacity of RC structures. The change is more evident when the applied electric field is larger or the operation period is longer.

A hydrogen evolution reaction may occur at the steel surface when applying ECC, which may cause the hydrogen embrittlement of the reinforcing steel, especially in pre-stressed concrete structures. Hence, to avoid hydrogen embrittlement in CP for RC structures, EN ISO 12696:2016 [32] stipulates that the 'instantaneous OFF' potential should be more positive than -1100 mV with respect to Ag/AgCl/0.5 M KCl for plain reinforcing steel and -900 mV for pre-stressed steel. Siegwart et al. [118] conducted an ECR for 22 pre-stressed concrete specimens, and found that the risk of hydrogen embrittlement could barely avoided regardless of the adjustment of the applied current density and the operation period of ECR. Recently, Mao et al. [119] reported that bidirectional electro-migrations could lower the risk of hydrogen embrittlement by adding triethylenetetramine into the external electrolyte solution, and found that the risk of hydrogen embrittlement could be neglected even with the applied current density of 3 A/m^2 for 14 d.

Compared with ECR and ER, it is clear that the adverse effects of CP on RC structures, including the bonding strength of the steel–concrete interface and the risk of hydrogen embrittlement, are almost neglected. In addition, the investigations by O'Flaherty et al. [114] indicated that ICCP could prevent chloride penetration or reduced chloride concentration in concrete. Christodoulou et al. [120] applied ICCP to control the corrosion of approximately 700 crossbeams in Midland Links Motorway Viaducts over the last 20 years. It was discovered that all the reinforcing steels in the beams remained in the passive state without ICCP for 24 months after the end of a 5-year. Therefore, a long-term ICCP can achieve ECR and ER.

6. DISCUSSION

Both ECR and ER aim to control the kinetic factors that induce the corrosion of RC structures, i.e., chloride ion and pH value. They have great advantages of short period, simple device and no space occupation. However, they have three significant disadvantages: (1) because the applied electric field is larger, the risk of hydrogen embrittlement of reinforcing steel is higher, and the effect on the bond strength of the steel-concrete interface is more significant; (2) because the treatment period is shorter, chloride ions that are physically and chemically bound by cement hydrates cannot be released timely, leading to that the efficiency of ECR is lower than expected; (3) they may be unsuitable for repairing highly corroded RC structures. Compared with ECR and ER, a well-designed CP has less influence on the interfacial bond strength and has less probability to cause the hydrogen embrittlement. Additionally, the long-term operation of CP can also improve the pH value adjacent to the reinforcing steel and lowers the concentration of chloride ions in concrete. However, the long-term operation of

CP can accelerate the consumption of anode system, lowering the service life [121, 122]. Therefore, the long-term ECC with an intermittent CP electric current [123] is an attractive approach to control the corrosion of RC structures, and it can achieve CP, ECR and ER. In this method, the electric current is switched on when the reinforcing steel tends to be corroded; the electric current is switched off when the chloride concentration at the steel surface is decreased to be lower than the threshold or the pH value of carbonated concrete is improved to be higher than 12. The numerical model of multispecies transport in RC with ECC can predict the ionic concentrations and the pH value, and is an important theoretical tool to investigate or design an intermittent ECC. The thermodynamic equilibrium between pore solution and cement hydrates can accurately express the relationship between free and bound chlorides [82, 91-93]. Additionally, the nonlinear polarization boundary at the steel–concrete interface must be considered when applying an intermittent ECC. Moreover, the moisture has a significant influence on the ionic transport for unsaturated concrete, and the oxygen concentration at the steel surface directly determines electrode reactions [60]. Therefore, it is imperative to develop the numerical model of ECC that includes ionic transport in pore solution, oxygen and moisture transports, thermodynamic reactions, and electrode kinetics.

In recent years, the corrosion monitoring technology of RC structures [124-128] and the artificial intelligence in civil engineering [129] have been rapidly developed. Considering that a small external electric field needs to be actively and periodically applied to RC structures in an intermittent ECC, the intelligent system that integrates the corrosion monitoring technology and the intermittent ECC will be possible in the future. Firstly, the embedded sensor and wireless communication technology, and the application of wireless ad hoc network make it possible to build a real-time monitoring and controlling intelligent platform [124, 130]. Additionally, as heterogeneous source technologies have already been matured, such as solar energy, wind energy, vibration energy, and corrosion energy [14, 128], the integrated system with self-collection energy can power for corrosion monitoring and control, and this greatly improves the field applicability of the system. Moreover, the corrosion state of reinforcing steel can be automatically distinguished by the corrosion monitoring technology, which can guide to design ECC. After applying the ECC, the corrosion control effect can be periodically and automatically evaluated, which is beneficial for timely adjusting the ECC (e.g. the position of anode, the amplitude and switching cycle of applied electric field, etc.). Therefore, considering that the degradation in the durability of RC owing to the corrosion is increasingly severe, particularly in some industrialized countries, the intelligent system integrating corrosion monitoring and ECC will be very necessitated.

7. CONCLUSIONS

ECC, i.e. CP, ECR or ER is the most direct and effective method to improve the durability of RC structures that are vulnerable to chloride or carbonation attacks. However, their function is only limited to corrosion control. Therefore, multifunctional ECC should be developed. For example, some electro-migrating corrosion inhibitors can penetrate to the steel surface with the help of the applied electric field of ECC, thereby yielding multiple corrosion control; developing the electro-thermal effect

of cement-base conductive anodes is to melt ice or snow; ECC with CFRP anodes achieves both corrosion control and structural reinforcement, and it will be an available approach to improve the safety and durability of RC structures with sever corrosion. Long-term ECC with an intermittent small current can achieve CP, ECR and ER, as well as overcome their shortcomings. Hence, this is an attractive approach to improve the durability of RC structures; additionally, it is imperative to develop a numerical model of ECC that includes ionic transport in the pore solution, oxygen and moisture transports, thermodynamic reactions, and electrode kinetics.

With the rapid developments of corrosion monitoring technology and artificial intelligence, an intelligent system that integrates corrosion monitoring technology and intermittent ECC will be enable in civil engineering in the future. As the corrosion of RC structures is increasingly severe, this intelligent system will be necessitated.

DECLARATION OF COMPETING INTEREST

The authors declare that they have no known competing financial interests or personal relationships that could have appeared to influence the work reported in this paper.

ACKNOWLEDGMENTS

The authors are grateful for the financial support of the National Key Research and Development Program of China (Project No.: 2017YFC0703410 and 2018YFC0809400) and the Nature Science Foundation of China (NSFC) (Project No.: 51908453 and 51578190).

References

1. C.L. Page and K.W.J. Treadaway, *Nature* 297 (1982) 109-1982.
2. C.L. Page and M.M. Page, Woodhead Publishing in Materials, (2007) England.
3. Q. Liu, D. Easterbrook, L. Li and D. Li, *Mag. Concrete Res.*, 69 (2017) 134-144.
4. Q. Liu, G. Feng, J. Xia, J. Yang and L. Li, *Compos. Struct.*, 183 (2018) 371-380.
5. Q. Liu, D. Easterbrook, J. Yang and L. Li, *Eng. Struct.*, 86 (2015) 122-133.
6. U.M. Angst and B. Elsener, *Sci. Adv.*, 3 (2017) e17007518.
7. X. Shi, N. Xie, K. Fortune and J. Gong, *Constr. Build. Mater.*, 30 (2012) 125-138.
8. U. Angst, B. Elsener, C.K. Larsen and Ø. Vennesland, *Cem. Concr. Res.*, 39 (2009) 1122-1138.
9. M. Stefanoni, U.M. Angst and B. Elsener, *Nat. Mater.*, 18 (2019) 942-947.
10. Z. Shi, B. Lothenbach, M.R. Geiker, J. Kaufmann, A. Leemann, S. Ferreiro and J. Skibsted, *Cem. Concr. Res.*, 88 (2016) 60-72.
11. A. Leemann and F. Moro, *Mater. Struct.*, 50 (2017) 1-14.
12. X. Shen, W. Jiang, D. Hou, Z. Hu, J. Yang and Q. Liu, *Cem. Concr. Compos.*, 104 (2019) 103402.
13. J. Liu, Q. Qiu, X. Chen, F. Xing, N. Han, Y. He and Y. Ma, *Cem. Concr. Res.*, 95 (2017) 217-225.
14. G. Qiao, G. Sun, H. Li and J. Ou, *Appl. Energ.*, 131 (2014) 87-96.
15. J. Ozbolt, G. Balabanic and M. Kuster, *Corros. Sci.*, 53 (2011) 4166-4177.
16. A. Goyal, H.S. Pouya, E. Ganjian and P. Claisse, *Arab. J. Sci. Eng.*, 43 (2018) 5035-5055.
17. M. Daniyal and S. Akhtar, *Journal of Building Pathology and Rehabilitation*, 1 (2020) 1-20.
18. C. Christodoulou, C. Goodier and G. Glass, *MATEC Web of Conferences*, 199 (2018) 5001.
19. L. Bertolini, M. Carsana, M. Gastaldi, F. Lollini and E. Redaelli, *Mater. Corros.*, 62 (2011) 146-154.

20. I. Martinez, F. Rozas, S. Ramos-Cillan, M. Gonzalez and M. Castellote, *Electrochim. Acta*, 181 (2015) 288-300.
21. T. Huang, X. Huang and P. Wu, *Int. J. Electrochem. Sc.*, (2014) 4589-4597.
22. T.Y. Hao, Y.Q. Su, Y. Li and H. Lin, *IOP Conference Series: Materials Science and Engineering*, 479 (2019) 12086.
23. L.B. Yu, L.H. Jiang, H.Q. Chu, M.Z. Guo, Z.Y. Zhu and H. Dong, *Constr. Build. Mater.,* 220 (2019) 538-546.
24. K. Wilson, M. Jawed and V. Ngala, *Constr. Build. Mater.*, 39 (2013) 19-25.
25. A. Byrne, N. Holmes and B. Norton, *Mag. Concrete Res.*, 13 (2016) 664-677.
26. U.M. Angst, *Corrosion Journal Org* 12 (2019) 1420-1433.
27. J.M. Miranda, A. Cobo, E. Otero and J.A. González, *Cem. Concr. Res.*, 37 (2007) 596-603.
28. S. Laurens and R. Francois, *RILEM Technical Letters*, (2017) 27-32.
29. Y. Liu and X. Shi, *Rev. Chem. Eng*., (2009) 339-388.
30. L. Bertolini, M. Gastaldi, M. Pedeferri and E. Redaelli, *Corros. Sci.*, 44 (2002) 1497-1513.
31. J. Carmona Calero, M.A. Climent Llorca and P. Garcés Terradillos, *J. Electroanal. Chem.*, 793 (2017) 8-17.
32. BS EN ISO 12696:2016, (2012) BSI Standards
33. J. Hou and D. Chung, *Cem. Concr. Res.*, 27 (1997) 649-656.
34. G. Qiao, B. Guo, Y. Hong and J. Ou, *Int. J. Electrochem. Sc.*, (2015) 8426-8436.
35. L. Bertolini, F. Bolzoni, T. Pastore and P. Pedeferri, *Cem. Concr. Res.*, 34 (2004) 681-694.
36. J. Xu and W. Yao, *Constr. Build. Mater.*, 25 (2011) 2655-2662.
37. M.S. Anwar, B. Sujitha and R. Vedalakshmi, *Constr. Build. Mater.*, 71 (2014) 167-180.
38. J. Carmona, P. Garcés and M.A. Climent, *Corros. Sci.*, 96 (2015) 102-111.
39. A. Cañón, P. Garcés, M.A. Climent, J. Carmona and E. Zornoza, *Corros. Sci.*, 77 (2013) 128-134.
40. A. Pérez, M.A. Climent and P. Garcés, *Corros. Sci.*, 52 (2010) 1576-1581.
41. Z. Jin, D. Hou and T. Zhao, *Constr. Build. Mater.*, 173 (2018) 149-159.
42. J. Hu, Y. Wang, Y. Ma, J. Wei and Q. Yu, *Math. Biosci. Eng.*, 6 (2019) 7510-7525.
43. J. Hu, Y. Wang, Z. Zhang, W. Guo, Y. Ma, W. Zhu, J. Wei and Q. Yu, *Constr. Build. Mater.*, 229 (2019) 116869.
44. W. Guo, J. Hu, Y. Ma, H. Huang and Q. Yu, *Corros. Sci.*, (2019) (In Press) https://doi.org/10.1016/j.corsci.2019.108366
45. B. Han, S. Sun, S. Ding, L. Zhang, X. Yu and J. Ou, *Compos. Part A-Appl. S.*, 70 (2015) 69-81.
46. B. Han, L. Zhang and J. Ou, *Journal of Wuhan University of Technology-Mater. Sci. Ed.*, 25 (2010) 147-151.
47. J. Chiou, Q. Zheng and D.D.L. Chung, *Composites* 20 (1989) 379-381.
48. Y. Dai, M. Sun, C. Liu and Z. Li, *Cem. Concr. Compos.*, 32 (2010) 508-513.
49. H. Li, H. Xiao and J. Ou, *Cem. Concr. Compos.*, 28 (2006) 824-828.
50. Y. Wang, G. Chen, B. Wan, G. Cai and Y. Zhang, *Constr. Build. Mater.*, 232 (2020) 117287.
51. S. Gadve, A. Mukherjee and S.N. Malhotra, *Corrosion-US* 2 (2011) 1-11.
52. S. Gadve, A. Mukherjee and S.N. Malhotra, *ACI Mater. J.*, 107 (2010) 349.
53. C. Van Nguyen, P. Lambert, P. Mangat, F. O Flaherty and G. Jones, *ISRN Corrosion* (2012) 1-9.
54. J.H. Zhu, M. Zhu, N. Han, W. Liu and F. Xing, *Materials (Basel)* 7 (2014) 5438-5453.
55. J. Zhu, M. Su, J. Huang, T. Ueda and F. Xing, *Constr. Build. Mater.*, 167 (2018) 669-679.
56. P. Lambert, C. Van Nguyen, P.S. Mangat, F.J. O Flaherty and G. Jones, *Mater. Struct.*, 48 (2015) 2157-2167.
57. M. Su, L. Wei, J. Zhu, T. Ueda, G. Guo and F. Xing, *J. Compos. Constr.,* 23 (2019) 04019021.
58. G. Qiao, B. Guo and J. Ou, Communication and Control. IEEE, (2015) Qinhuangdao.
59. G. Qiao, B. Guo and J. Ou, *J. Mater. Civil Eng.*, 29 (2017) (6) -1--1
60. E.B. Muehlenkamp, M.D. Koretsky and J.C. Westall, *Corrosion-US* 61 (2005) 519-533.
61. G. Qiao, B. Guo, J. Ou, F. Xu and Z. Li, *Constr. Build. Mater.*, 119 (2016) 260-267.

62. A.M. Hassanein, G.K. Glass and N.R. Buenfeld, *Cem. Concr. Compos.*, 24 (2002) 159-167.
63. M.M.S. Cheung and C. Cao, *Constr. Build. Mater.*, 45 (2013) 199-207.
64. S. Fonna, S. Huzni and A. Zaim, *Journal of Mechanical Engineering* 2 (2017) 111-122.
65. M. Bruns and M. Raupach, *Mater. Corros.*, 61 (2010) 505-511.
66. Y. Liu and X. Shi, *Anti-Corros. Method. M.*, 59 (2012) 121-131.
67. NACE Standard TM0294-2007, (2007) USA, No. 21225.
68. T. Bennett, W. David and L. Lankard, Strategic Highway Research Program, National Academy of Sciences, 2101 Constitution Avenue N.W., Washington, DC 204181993.
69. T. Ueda, K. Wakitani and A. Nanasawa, *Electrochim. Acta*, 86 (2012) 23-27.
70. W. Yodsudjai and W. Saelim, *J. Mater. Civil Eng.*, 1 (2014) 83-89.
71. H. The, A. Tuan, L. Van Khu, M. Thi, T. Hoang and X. Shi, *Anti-Corros. Method. M.*, 63 (2016) 377-385.
72. H. Shan, J. Xu, Z. Wang, L. Jiang and N. Xu, *Constr. Build. Mater.*, 127 (2016) 344-352.
73. L.R. de Almeida Souza, M.H.F. de Medeiros, E. Pereira and A.P.B. Capraro, *Constr. Build. Mater.*, 145 (2017) 435-444.
74. K.B. Kim, J.P. Hwang and K.Y. Ann, *Constr. Build. Mater.*, 104 (2016) 191-197.
75. P. Garcés, M.J. Sánchez De Rojas and M.A. Climent, *Corros. Sci.*, 48 (2006) 531-545.
76. C.C. Chang, W. Yeih, J.J. Chang and R. Huang, C*onstr. Build. Mater.*, 68 (2014) 692-700.
77. W. Yeih, J.J. Chang, C.C. Chang, K.L. Chen and M.C. Chi, *Cem. Concr. Compos.*, 74 (2016) 136-146.
78. V. Saraswathy, H. Lee, S. Karthick and S. Kwon, *Constr. Build. Mater.*, 158 (2018) 549-562.
79. G. Fajardo, G. Escadeillas and G. Arliguie, *Corros. Sci.*, 48 (2006) 110-125.
80. J.C. Orellan, G. Escadeillas and G. Arliguie, *Cem. Concr. Res.*, 34 (2004) 227-234.
81. Q. Yuan, C. Shi, G. De Schutter, K. Audenaert and D. Deng, *Constr. Build. Mater.*, 23 (2009) 1-13.
82. B. Guo, Y. Hong, G. Qiao, J. Ou and Z. Li, *J. Colloid Interf. Sci.*, 531 (2018) 56-63.
83. B. Elsener and U. Angst, *Corros. Sci.*, 49 (2007) 4504-4522.
84. M. Siegwart, J.F. Lyness and B.J. McFarland, Cem. Concr. Res., 33 (2003) 1211-1221.
85. Y.T.N. Hai, W. Pansuk and P. Sancharoen, KSCE J. Civ Eng 22 (2018) 2942-2950.
86. J.M. Miranda, J.A. González, A. Cobo and E. Otero, *Corros. Sci.*, 48 (2006) 2172-2188.
87. T.Y. Hao, H. Lin, Y. Li and C. Zhao, *IOP Conf. Series: Materials Science and Engineering* (2019) 012031.
88. J. Zhu, L. Wei, Z. Wang, L.C. Ke, Y. Fang and F. Xing, *Constr. Build. Mater.*, 120 (2016) 275-283.
89. Y. Li, X. Liu, M. Wu and W. Bai, *Constr. Build. Mater.*, 153 (2017) 436-444.
90. H. Lin, Y. Li and Y. Li, *Constr. Build. Mater.*, 197 (2019) 228-240.
91. Y. Elakneswaran, A. Iwasa, T. Nawa, T. Sato and K. Kurumisawa, *Cem. Concr. Res.*, 40 (2010) 1756-1765.
92. B. Lothenbach, D.A. Kulik, T. Matschei, M. Balonis, L. Baquerizo, B. Dilnesa, G.D. Miron and R.J. Myers, *Cem. Concr. Res.*, 115 (2019) 472-506.
93. B. Lothenbacha and M. Zajac, *Cem. Concr. Res.*, 123 (2019) 105779.
94. O.B. Isgor and W.J. Weiss, *Mater. Struct.*, 52 (2019) 1-17.
95. T. Van Quan, A. Soive, S. Bonnet and A. Khelidj, *Constr. Build. Mater.*, 191 (2018) 608-618.
96. V.Q. Tran, A. Soive and V. Baroghel-Bouny, *Cem. Concr. Res.*, 110 (2018) 70-85.
97. B. Guo, Y. Hong, G. Qiao and J. Ou, *Constr. Build. Mater.*, 187 (2018) 839-853.
98. Y. Wang, L.Y. Li and C.L. Page, *Comp. Mater. Sci.*, 20 (2001) 196-212.
99. L.Y. Li and C.L Page, *Corros. Sci.*, 42 (2000) 2145-2165.
100. L.Y. Li and C.L Page, *Comp. Mater. Sci.*, 9 (1998) 303-308.
101. A. Toumi, R. François and O. Alvarado, *Cem. Concr. Res.*, 37 (2007) 54-62.
102. S. Jin, J. Xia, W. Jin, Z. Yu, J. Hu, Q. Lyu and X. Zhong. Sixth International Conference on Durability of Concrete Structures, (2018) University of Leeds.

103. J. Xia, Q. Liu, J. Mao, Z. Qian, S. Jin, J. Hu and W. Jin, *Constr. Build. Mater.*, 193 (2018) 189-195.
104. J. Xia and L. Li, *Constr. Build. Mater.*, 39 (2013) 51-59.
105. J. Xu and F. Li, *Ocean Eng.*, 179 (2019) 38-50.
106. Q. Liu, L. Li, D. Easterbrook and J. Yang, *Eng. Struct.*, 42 (2012) 201-213.
107. Q. Liu, J. Xia, D. Easterbrook, J. Yang and L. Li, *Constr. Build. Mater.*, 70 (2014) 410-427.
108. L. Bertolini, M. Carsana and E. Redaelli, *J. Cult. Herit.*, 9 (2008) 376-385.
109. W. Yeih and J.J. Chang, *Constr. Build. Mater.*, 19 (2005) 516-524.
110. Y. Tong, V. Bouteiller, E. Marie-Victoire and S. Joiret, *Cem. Concr. Res.*, 42 (2012) 84-94.
111. P.H.L.C. Ribeiro, G.R. Meira, P.R.R. Ferreira and N. Perazzo, *Constr. Build. Mater.*, 40 (2013) 280-290.
112. E. Redaelli and L. Bertolini, *J. Appl. Electrochem.*, 41 (2011) 817-827.
113. L. Mao, Z. Hu, J. Xia, G. Feng, I. Azim, J. Yang and Q. Liu, *Compos. Struct.*, 207 (2019) 176-189.
114. F. O'Flaherty, C. Van Nguyen, P. Lambert, P. Mangat and G. Jones, *Mater. Corros.*, (2018) 1-12.
115. J. Garcia, F. Almeraya, C. Barrios, C. Gaona, R. Nunez, I. Lopez, M. Rodriguez, A. Martinez-Villafane and J.M. Bastidas, *Cem. Concr. Compos.*, 34 (2012) 242-247.
116. Q. Zhang and J. Gong, *Constr. Build. Mater.*, 50 (2014) 549-559.
117. Y. Guo. Dalian University of Technology, PhD thesis (2010) (in Chinese).
118. M. Siegwart, J.F. Lyness, B.J. McFarland and G. Doyle, Constr. Build. Mater., 19 (2005) 585-594.
119. J. Mao, W. Jin, J. Zhang, J. Xia, W. Fan and Y. Xu, *Constr. Build. Mater.*, 213 (2019) 582-591.
120. C. Christodoulou, G. Glass, J. Webb, S. Austin and C. Goodier, *Corros. Sci.*, 52 (2010) 2671-2679.
121. T. Paul and P.E. Teng, (2011) Department of Transportation Federal Highway Administration (FHWA).
122. A.A. Sohanghpurwala and W. Scannell, (2003) U.S. Department of Transportation Federal Highway Administration Research and Development.
123. D. Stephen, S.J. Cramer, B.S. Bullard, J. Covino, M. Ziomek-Moroz and G.R. Holcomb, (2005) Federal Highway Administration Washington, D.C.
124. G. Sun, G. Qiao and B. Xu, *IEEE Sens. J.*, 11 (2011) 1476-1477.
125. G. Qiao, Y. Hong, G. Song, H. Li and J. Ou, *Sensor. Actuat. B-Chem.*, 168 (2012) 172-177.
126. T. Liu and G. Qiao, *IEEE Sens. J.*, 11 (2011) 2111-2112.
127. G. Qiao and J. Ou, *Electrochim. Acta*, 52 (2007) 8008-8019.
128. W. Guo, X. Li, M. Chen, L. Xu, L. Dong, X. Cao, W. Tang, J. Zhu, C. Lin, C. Pan and Z.L. Wang, *Adv. Funct. Mater.*, 24 (2014) 6691-6699.
129. Y. Bao and H. Li, *China Civil Engineering Journal*, 52 (2019) 1-11.
130. Y. Yu, G. Qiao and J. Ou, *IEEE Sens. J.*, 10 (2010) 1901-1902